2002

Advances in Space Radiation Shielding Codes

John W. Wilson

Ram K. Tripathi

Garry D. Qualls

Francis A. Cucinotta

Richard E. Prael

See next page for additional authors

Original Publication Citation

Wilson, J. W., Tripathi, R. K., Qualls, G. D., Cucinotta, F. A., Prael, R. E., Norbury, J. W., . . . De Angelis, G. (2002). Advances in space radiation shielding codes. *Journal of Radiation Research, 43*, S87-S91. doi:10.1269/jrr.43.S87

J. RADIAT. RES., 43: SUPPL., S87–S91 (2002)

Advances in Space Radiation Shielding Codes

JOHN W. WILSON[1]*, RAM K. TRIPATHI[1], GARRY D. QUALLS[1],
FRANCIS A. CUCINOTTA[2], RICHARD E. PRAEL[3],
JOHN W. NORBURY[4], JOHN H. HEINBOCKEL[5],
JOHN TWEED[5] and GIOVANNI DE ANGELIS[5]

Space / Radiation / High-energy ions

Early space radiation shield code development relied on Monte Carlo methods and made important contributions to the space program. Monte Carlo methods have resorted to restricted one-dimensional problems leading to imperfect representation of appropriate boundary conditions. Even so, intensive computational requirements resulted and shield evaluation was made near the end of the design process. Resolving shielding issues usually had a negative impact on the design. Improved spacecraft shield design requires early entry of radiation constraints into the design process to maximize performance and minimize costs. As a result, we have been investigating high-speed computational procedures to allow shield analysis from the preliminary concept to the final design. For the last few decades, we have pursued deterministic solutions of the Boltzmann equation allowing field mapping within the International Space Station (ISS) in tens of minutes using standard Finite Element Method (FEM) geometry common to engineering design methods. A single ray trace in such geometry requires 14 milliseconds and limits application of Monte Carlo methods to such engineering models. A potential means of improving the Monte Carlo efficiency in coupling to spacecraft geometry is given.

INTRODUCTION

The interaction of radiation with materials is of importance to understanding our environment[1)] and in the application of health based procedures[2)]. Early methods of space radiation shield evaluation relied largely on Monte Carlo codes[3,4)] and made important contributions to NASA engineering programs such as Apollo, Lunar Orbiter, Viking, Supersonic Transport[5)], High Speed Civil Transport[6)]… Yet, slow computational procedures did not allow early entry of radiation constraints into the design process and off-optimum solutions to shielding problems continue to plague final designs[7,8)]. Even today, simulations with full 3D Monte Carlo codes often use methods with questionably simplified shielding geometry to increase computational speed in which, for example, ISS is approximated as a 20.7 g/cm^2 thick aluminum cylindrical shell[9)] leading to an overestimate of the neutron flux within ISS since neutron leakage is minimal in this configuration. The use of a 3D Monte Carlo code within such a simplified geometry will lead to erroneous overestimates of the charged particle shielding since anisotropic shield distributions within ISS are known to be a major factor in astronaut exposure estimates[10)]. The development of high-speed computational procedures allows early entry of radiation constraints into the design optimization process[11)] and Monte Carlo methods should still play a role in final design evaluation with full optimized geometry. This is especially true with the recent advances of the LAHET Monte Carlo code with addition of nucleus-nucleus reactions under the ISABEL nuclear reaction option[12–14)] and planned extensions. We examine herein the errors introduced by the simplifying models used with

*Corresponding author: Phone: +1–757–864–1414
Fax: +1–757–864–8094
E-mail: john.w.wilson@larc.nasa.gov
[1] NASA Langley Research Center, Hampton, VA 23681 USA
[2] NASA Johnson Space Center, Houston, TX 77058 USA
[3] Los Alamos National Laboratory, Los Alamos, NM 87545 USA
[4] University of Wisconsin-Milwaukee, Milwaukee, WI 53201 USA
[5] Old Dominion University, Norfolk, VA 23529 USA

Monte Carlo codes and propose a method of resolving the current inefficient coupling of Monte Carlo methods to engineering models.

DETERMINISTIC METHOD

The relevant transport equations are the linear Boltzmann equations for the flux density $\phi_j(\boldsymbol{x},\boldsymbol{\Omega},E)$ for particle type j and are written as

$$\boldsymbol{\Omega}\bullet\boldsymbol{\nabla}\phi_j(\boldsymbol{x},\boldsymbol{\Omega},E) = \sum\int \sigma_{jk}(\boldsymbol{\Omega},\boldsymbol{\Omega}',E,E')\phi_k(\boldsymbol{x},\boldsymbol{\Omega}',E')\,d\boldsymbol{\Omega}'\,dE' - \sigma_j(E)\,\phi_j(\boldsymbol{x},\boldsymbol{\Omega},E) \quad (1)$$

where $\sigma_j(E)$ and $\sigma_{jk}(\boldsymbol{\Omega},\boldsymbol{\Omega}',E,E')$ are the shield media macroscopic cross sections. The $\sigma_{jk}(\boldsymbol{\Omega},\boldsymbol{\Omega}',E,E')$ represent all those processes by which type k particles moving in direction $\boldsymbol{\Omega}'$ with energy E' produce a type j particle in direction $\boldsymbol{\Omega}$ with energy E (*including decay processes*). Note that there may be several reactions that produce a particular product, and the appropriate cross sections for equation (1) are the inclusive ones. Exclusive processes are functions of the particle fields and may be evaluated once the particle fields are known. The total cross section $\sigma_j(E)$ for the medium for each particle type is

$$\sigma_j(E) = \sigma_{j,at}(E) + \sigma_{j,el}(E) + \sigma_{j,r}(E) \quad (2)$$

where the first term refers to collision with atomic electrons, the second term is for elastic nuclear scattering, and the third term describes nuclear reactions where we have ignored the minor nuclear inelastic processes. The corresponding differential cross section $\sigma_{jk}(\boldsymbol{\Omega},\boldsymbol{\Omega}',E,E')$ is similarly delineated (note, $k = j$ for atomic and elastic processes). Many atomic collisions ($\sim 10^6$) occur in a centimeter of ordinary matter, whereas $\sim 10^3$ nuclear coulomb elastic collisions occur per centimeter, while nuclear reactions are separated by a fraction to many centimeters depending on energy and particle type. Solutions use the atomic collisions as first perturbation with special methods used for neutrons for which atomic cross-sections are taken as zero. The solution of equation (1) involves hundreds of multi-dimensional integro-differential equations that are coupled together by thousands of energy dependent cross terms and must be solved self-consistently subject to boundary conditions.

The nuclear reactive cross sections can be written in the following form

$$\sigma_{jk,r}(\boldsymbol{\Omega},\boldsymbol{\Omega}',E,E') = \sigma_{jk,iso}(E,E') + \sigma_{jk,for}(\boldsymbol{\Omega},\boldsymbol{\Omega}',E,E') \quad (3)$$

where the first term is isotropic and associated with lower energy particles produced including target fragments and the second term is highly peaked in the forward direction and is associated mainly with direct quasi-elastic events, charge exchange, and projectile fragments. Surprisingly even nucleon-induced reactions follow this simple form and the isotropic term extends to relatively high energies[15]. As an example of nucleon induced reactions, the following form has been used in versions of FLUKA[15] as follows

$$\sigma_{jk,r}(\boldsymbol{\Omega},\boldsymbol{\Omega}',E,E') = \nu_{jk}(E')\sigma_{jkr}(E')f_{jk}(E,E')g_R(\boldsymbol{\Omega}\bullet\boldsymbol{\Omega}',E,A_T) \quad (4)$$

where the Ranft factor used in early versions of FLUKA is

$$g_R(\boldsymbol{\Omega}\bullet\boldsymbol{\Omega}',E,A_T) = N_R\,exp[-\theta^2/\lambda_R] \quad \pi/2 \geq \theta \geq 0 \quad (5)$$

and constant for larger values of production angle θ and λ_R given by Ranft as

$$\lambda_R = (0.12 + 0.00036A_T/E) \quad (6)$$

although new generalized fits are being derived. This separation in phase space is exploited in the present HZETRN code for efficient computational procedures and contributes to the neutron albedo.

Atomic interactions limit the contributions of charged particles in the transport process. For example, the protons and alpha particles produced in aluminum below 100 A MeV contribute to the fluence only within a few centimeters of their collision source and the heavier ions are even more restricted. This is an important factor in that the transported secondary charged particle flux tends to be small at low energies and the role of additional nuclear reactions are likewise limited.

We rewrite equation (1) in operator notation in which the field functions $\phi_j(\boldsymbol{x},\ \boldsymbol{\Omega},\ E)$ are combined in a vector array $\boldsymbol{\Phi}$ as

$$\boldsymbol{\Phi} = [\phi_j(\boldsymbol{x},\boldsymbol{\Omega},E)] \quad (7)$$

with the drift term replaced by a diagonal matrix operator as

$$\boldsymbol{D} = [\boldsymbol{\Omega}\bullet\boldsymbol{\nabla}] \quad (8)$$

and the interaction kernel into an operator containing diagonal $[\sigma_j(E)]$ and lower triangular elements related to $\sigma_{jk}(\boldsymbol{\Omega},\boldsymbol{\Omega}',E,E')$ given as

$$\boldsymbol{I} = [\Sigma\int \sigma_{jk}(\boldsymbol{\Omega},\boldsymbol{\Omega}',E,E')\,d\boldsymbol{\Omega}'\,dE' - \sigma_j(E)] \quad (9)$$

The interaction operator $\boldsymbol{I}$ has three parts associated with atomic, elastic, and reactive processes as given in equation (2). Equation (1) is then rewritten with each contribution (atomic, elastic, reactive) shown separately as

$$[\boldsymbol{D} - \boldsymbol{I}_{at} - \boldsymbol{I}_{el}]\bullet\boldsymbol{\Phi} = \boldsymbol{I}_r\bullet\boldsymbol{\Phi} \quad (10)$$

where the first two physical perturbation terms (also diagonal operators) are shown on the left-hand side and have been

adequately resolved in past research. The reaction cross section is separated by equation (3) into isotropic and forward components for which equation (10) may be written as coupled equations

$$[D - I_{at} - I_{el} + \sigma_r]\bullet\Phi_{for} = \{\int \sigma_{r,for}(\Omega,\Omega',E,E')\, d\Omega'\, dE'\}\bullet \Phi_{for} \equiv \Xi_{r,for}\, \Phi_{for} \quad (11)$$

and

$$[D - I_{at} - I_{el} + \sigma_r]\bullet\Phi_{iso} = \{\int \sigma_r(\Omega,\Omega',E,E')\, d\Omega'\, dE'\}\bullet\Phi_{iso} + \{\int \sigma_{r,iso}(E,E')\, d\Omega'\, dE'\}\bullet\Phi_{for} \equiv \Xi_r \bullet \Phi_{iso} + \Xi_{r,iso} \bullet \Phi_{for} \quad (12)$$

where $\Phi = \Phi_{for} + \Phi_{iso}$ and the operator Ξ_r is the integral portion of I_r. Equation (11) is a Volterra equation and can be solved as a Neuman series[16,17] which can be either evaluated directly or proscribed as a marching procedure in either a perturbative sense as the current form of HZETRN or nonperturbative sense (future version of HZETRN) as described elsewhere[18]. The cross term in equation (12) gives rise to an isotropic source of light ions and neutrons of only modest energies. Spectral contributions to the Neuman series depend on the particle range and probability of surviving nuclear reactions which establish the functional form of the G matrix ($G = [D - I_{at} - I_{el} + \sigma_r]^{-1}$) as the inverse of the differential operator on the left of equations (11) and (12). The second term of the Neuman series is proportional to the probability of nuclear reaction that is limited by the particle range as discussed above. It is well known that nuclear reactions for the charged particles below a few hundred A MeV are infrequent for which rapid convergence has been demonstrated[17].

The remaining problem is solution for the transport of the low-energy neutron and light ion isotropic sources in equation (12) that dominate the solution below about 70 A MeV. In this region light ion transport is completely dominated by the atomic interaction terms and only a very small fraction have nuclear reactions making only minor contributions to the particle fields. This is especially true for the target fragments, which can be solved in closed form[16,17].

The neutrons have no charge and are dominated at low energies by elastic and reactive nuclear processes. We further expand equation (12) for the single neutron component as

$$[\Omega\bullet\nabla + \sigma_n]\ \phi_n(x,\Omega,E) \equiv \int \sigma_{nn}(\Omega,\Omega',E,E')\ \phi_n(x,\Omega',E')\, d\Omega'\, dE' + [\Xi_{r,iso}\bullet\Phi_{for} + \Xi_r\bullet\Phi_{(12)}]_n \quad (13)$$

where the last term is from coupling to the solution of equation (12). The neutron spectrum is greatly degraded in energy on the first collision and what remains of the low-energy neutron transport is the last issue to be resolved. This is the typical nuclear engineering problem for which a multitude of methods have been developed such as the Sn, multigroup, and collocation methods already applied to versions of HZETRN. It is mainly a question of computational efficiency and we continue to investigate this issue. Monte Carlo methods have been helpful in evaluation of these computational procedures in simple geometry.

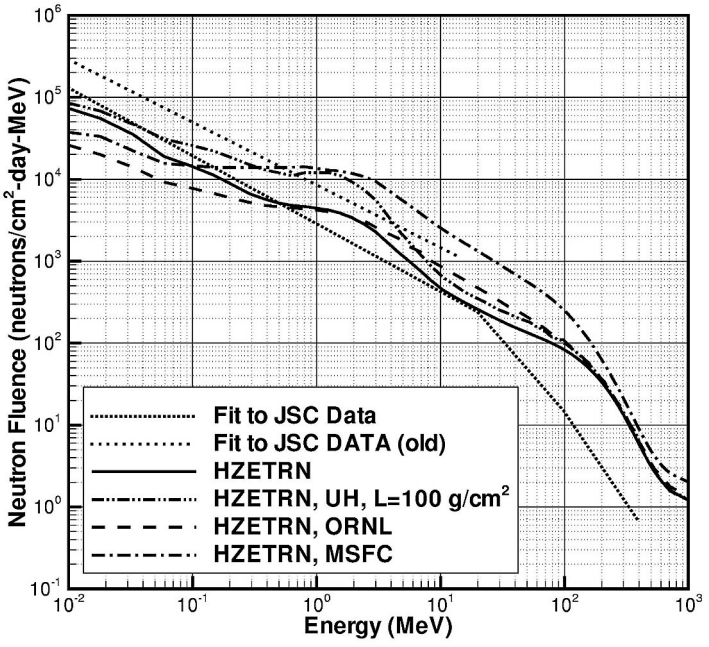

Fig. 1. Neutron spectra within the Shuttle on STS-36 with old and new fits to JSC Bonner sphere data.

ROLE OF BOUNDARY CONDITIONS

The deterministic HZETRN code (solving equation (13) by multigroup) is of sufficient generality to solve the simplified Shuttle geometry using the long cylindrical shell (MSFC)[9], the sector analysis (UH using a 100 g/cm^2 slab geometry)[19], spherical shell (ORNL)[20], and the actual Shuttle geometry (HZETRN)[8] during STS-36 with results for neutrons and protons shown in figures 1 and 2 respectively. The results of the Bonner sphere measurements of Johnson Space Center on STS-36 with the original analysis using a simple power-law spectrum (JSC old) and the new JSC analysis using a bimodal power-law spectrum[21] are shown in figure 1 for comparison. It is clear that the actual geometry matters and the actual geometry (HZETRN) seems the best approximation to the latest analysis (JSC) of the Bonner sphere data. There are similar large differences for the proton spectra as a function of boundary conditions as shown in figure 2. Prior comparison of calculated proton spectra with telescope measurements on STS-48 have validated the use of HZETRN with real geometry on Shuttle (see figure 3)[22].

The limitation of long computation times for ray tracing

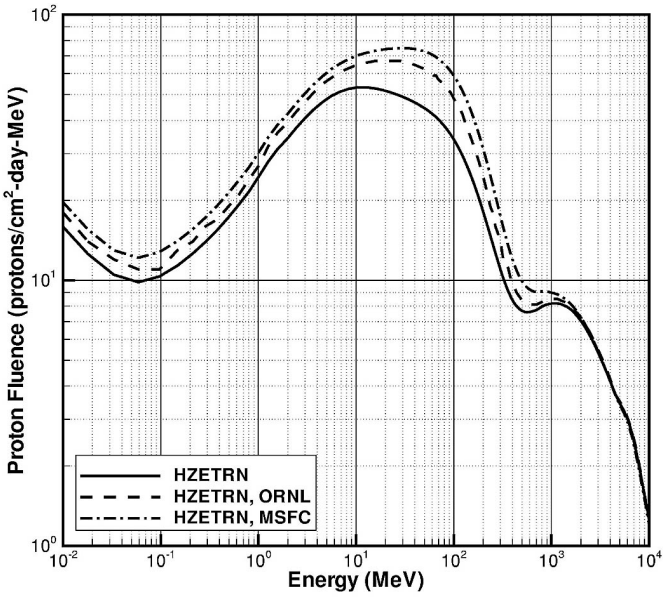

Fig. 2. Calculated proton spectra within the Shuttle on STS-36 according to various geometry models.

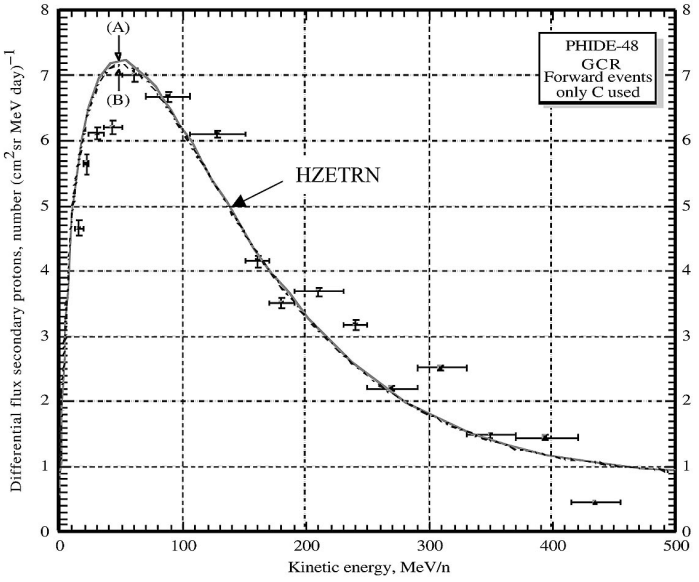

Fig. 3. Calculated and measured proton spectra produced within the Shuttle by GCR on STS-48.

in engineering FEM models which severely limits Monte Carlo application to ISS (14 msec per ray on a 16 processor Onyx2) has some hope of gaining performance on reconfigurable computers (Field Programmable Gate Arrays, or hypercomputer). This is a similar calculation as that done by high-performance video cards using Gate Arrays. These computers have massive inherent parallel capability able to search many facets in parallel and will be the focus of future research in support of implementing the multiple-charged ion transport Monte Carlo version of LAHET or the JAERI HZE version of HETC.

CONCLUSIONS

The primary limitation of Monte Carlo is the interface with large scale engineering FEM models which require an average 14 msec to process a single segment of a Monte Carlo history on a 16 processor Onyx2. An approach to high-speed Monte Carlo using hypercomputers is suggested as a means to make such calculations practical since megaprocessor scaleup of cpu based methods will likely fall short and is inordinately expensive. Deterministic methods have demonstrated high-speed computations on modest cpu based implementations enabling development of advanced engineering design methods and are reasonably validated with flight measurements and Monte Carlo simulations in simple geometry.

REFERENCES

1. Yasuda, H. and Fujitaka, K. (2001) Cosmic radiation protection dosimetry using an electronic personal dosemeter (Siemens EPD) on selected internal flights. J. Radiat. Res. **42**: 57–68.
2. Kramer, M. (2001) Treatment planning for heavy-ion radiotherapy: Biological optimization of multiple beam ports. J. Radiat. Res. **42**: 39–46.
3. Alsmiller, R. G. (1967) High-energy nucleon transport and space vehicle shielding. Nucl. Sci. & Eng. **27**: 158–189.
4. Lambiotte, J. J., Wilson, J. W. and Filippas, T. A. (1971) Proper-3C: A nucleon-pion transport code. NASA TM X2158.
5. Foelsche, T., Mendell, R. B., Wilson, J. W. and Adams, R. R. (1974) Measured and Calculated Neutron Spectra and Dose Equivalent Rates at High Altitudes, Relevance to SST Operations and Space Research. NASA TN D-7715.
6. Wilson, J. W., Nealy, J. E., Cucinotta, F. A. and Shinn, J. L. (1995) Radiation Safety Aspects of the High-Speed Civil Transport (HSCT), NASA TP-3524.
7. Aerospace Safety Advisory Panel (2000), www.hq.nasa.gov/office/codeq/codeq-1.htm
8. Qualls, G. D., Wilson, J. W., Sandridge, C. A., Cucinotta, F. A., Nealy, J. E., Heinbockel, J. H., Hugger, C., Verhage, J., Anderson, B. M., Atwell, W., Zapp, N. and Barber, R. (2001) International Space Station Shielding Model Development. SAE 2001-01-2370.
9. Armstrong, T. W. and Colburn, B. L. (2001) Predictions of secondary neutrons and their importance to radiation effects inside the international space station. Radiat. Meas. **33**: 229–234.
10. Wilson, J. W., Nealy, J. E., Wood, J. S., Qualls, G. D., Atwell, W., Shinn, J. L. and Simonsen, L. C. (1995) Variations in astronaut radiation exposure due to anisotropic shield distribution. Health Phys. **69**: 34–45.
11. Wilson, J. W. and Khandelwal, G. S. (1974) Proton dose approximation in convex geometry. Nucl. Tech. **23**: 298–305.
12. Clover, M. R., DeVries, R. M., DiGiacomo, N. J. and Yariv, Y. (1982), Phys. Rev. C**, 26**: 2138.
13. Prael, R. E. (1998) "Upgrading Physics Packages for LAHET/MCNPX", Proceedings of the 2nd International Topical Meeting on Nuclear Applications of Accelerator Technology, Gatlinburg, TN, September 20–23, 1998.
14. Prael, R. E. (2001) "Release Notes for LAHET Code System with LAHET Version 3.16", Los Alamos National Laboratory report LA-UR-01-1655.
15. Ranft, J. (1980) The FLUKA and KASPRO hadronic cascade codes. Computer Techniques in Radiation Transport and Dosimetry, W. R. Nelson and T. M. Jenkins, eds., Plenum Press, pp. 339–371.
16. Wilson, J. W. (1977) Analysis of the theory of high-energy ion transport. NASA TN D-8381.
17. Wilson, J. W., Townsend, L. W., Schimmerling, W., Khandelwal, G. S., Khan, F., Nealy, J. E., Cucinotta, F. A., Simonsen, L. C., Shinn, J. L. and Norbury, J. W. (1991) Transport Methods and Interactions for Space Radiations. NASA RP-1257.
18. Wilson, J. W., Shavers, M. R., Badavi, F. F., Miller, J., Shinn, J. L. and Costen, R. C. (1994) Nonperturbative Methods in HZE Propagation. Radiat. Res. **140**: 241–244.
19. Pinsky, L., Carminati, F. and Ferrari, A. (2001) Simulation of space Shuttle neutron measurements with FLUKA. Radiat. Meas. **33**: 335–339.
20. Alsmiller, R. G., Santoro, R. T., Barish, J. and Claiborne, H. C. (1972) Shielding of Manned Space Vehicles Against Protons and Alpha Particles. ORNL-RSIC-35.
21. Badhwar, G. D., Keith, J. E. and Cleghorn, T. F. (2001) Neutron measurements onboard the space shuttle. Radiat. Meas. **33**: 235–242.
22. Shinn, J. L., Cucinotta, F. A., Simonsen, L. C., Wilson, J. W., Badavi, F. F., Badhwar, G. D., Miller, J., Zeitlin, C., Heilbronn, L., Tripathi, R. K., Clowdsley, M. S., Heinbockel, J. H. and Xapsos, M. A. (1998) "Validation of a Comprehensive Space Radiation Transport Code", IEEE Transactions on Nuclear Science, **45**: 2711–2719.

Received on April 25, 2002
Revision on August 19, 2002
Accepted on November 13, 2002